Ultrafast Orientational Dynamics of Nanoconfined Benzene

Xiang Zhu, Richard A. Farrer, and John T. Fourkas*

Eugene F. Merkert Chemistry Center, Boston College, Chestnut Hill, Massachusetts 02467

Received: March 16, 2005; In Final Form: May 13, 2005

Ultrafast optical Kerr effect spectroscopy has been used to study the orientational dynamics of benzene and benzene-d_6 confined in nanoporous sol−gel glass monoliths with a range of average pore sizes. All of the observed orientational diffusion of confined benzene is found to occur on a slower time scale than in the bulk, even in pores with diameters that are significantly larger than a benzene molecule. The orientational dynamics of benzene-d_6 are found to be inhibited to a lesser extent than those of benzene, which is attributed to the differences in wetting properties of the two liquids on silica. The decays are fit well by a sum of two exponentials, the faster of which depends on pore size. Similar results are found in pores that have been modified with trimethylsilyl groups, although the relaxation is faster than in unmodified pores. Comparison to Raman line width data for confined benzene-d_6 suggests that the liquid exhibits significant structuring at the pore walls, with the benzene molecules lying flat on the surfaces of unmodified pores.

I. Introduction

Nanoconfinement can have a profound influence on the behavior of liquids.[1−5] The prevalence of liquids confined on molecular distance scales in science and technology has resulted in considerable effort being devoted to studying this problem. While significant progress has been made in understanding how nanoconfinement affects the structure and dynamics of liquids, there also remains much to be learned.

Our efforts in studying nanoconfined liquids have focused on using ultrafast spectroscopy to study the dynamics of liquids confined in porous sol−gel silicate glasses.[6−17] These materials are ideally suited for optical spectroscopy of nanoconfined liquids. Monoliths with high optical quality and high porosity can be fabricated readily in the laboratory.[18] The average pore size can be controlled synthetically, and the pore diameters are relatively monodisperse. In addition, the interactions between the pore surfaces and the confined liquid can be controlled via well-known surface-modification chemistry.[19]

Our method of choice for studying dynamics of liquids confined in sol−gel monoliths is optical Kerr effect (OKE) spectroscopy.[20−30] In this technique, a subpicosecond, linearly polarized pump pulse propagates through a transparent liquid composed of molecules with anisotropic polarizabilities, creating a slight net alignment of the molecules. This alignment creates a transient birefringence that can be monitored by a second, time-delayed probe pulse that is polarized at 45° relative to the pump pulse polarization. While a number of different factors contribute to the decay of the birefringence of the sample following excitation,[20−30] in our studies of nanoconfined liquids we are most interested in the slowest relaxation, which results from the orientational diffusion of molecules to return the liquid to an isotropic orientational state.

In previous studies we have found that even when the confined liquid only weakly wets the surfaces of the nanopores, its reorientational dynamics are still affected significantly.[6,7,9,11,17] In weakly wetting liquids composed of rodlike molecules, such as CS_2 or 2-butyne, multiexponential decays are observed.[6,7,11,17] The fastest of the exponentials has a decay constant that matches that of the bulk liquid, whereas the other exponentials can decay significantly more slowly. In the case of 2-butyne, we have observed a second exponential with a decay time that is exactly twice that of the bulk liquid, regardless of pore size, and a third, even slower decay that does depend on pore size.[17] Our interpretation of such data is that there is a population of molecules in the centers of the pores that is not affected by confinement and a second population at the pore surfaces that is affected in two ways. First, for reorientation off of the pore surfaces there is necessarily a factor of 2 increase in hydrodynamic volume, which accounts for the intermediate decay component. Second, reorientation along the pore surfaces is inhibited by geometric constraints, accounting for the pore-size dependent decay component. Furthermore, the thickness of the surface layer of molecules that have retarded orientational dynamics is less than a monolayer, which we believe is indicative of the fact that the orientational dynamics of molecules that lie normal to the pore surfaces are not influenced by their proximity to the pore walls.[11,16]

These proposed mechanisms for dynamic inhibition of weakly wetting liquids at pore surfaces rely upon the molecules being rodlike in nature. If the molecules are instead disk-shaped, it is not obvious that the same phenomena should be observed. For instance, reorientation about the axis of the disk should not necessarily be inhibited at pore surfaces, and so the geometric confinement effect might not be expected to exist for such liquids. Furthermore, the increase in hydrodynamic volume for reorientation should be smaller for disks rotating off of the surface of a pore than for cylinders. Here we investigate whether the same phenomena observed for weakly wetting liquids composed of rodlike molecules hold for benzene or benzene-d_6, both of which are composed of disk-shaped molecules that cannot hydrogen bond to silicate surfaces.

II. Experimental Section

Nanoporous sol−gel monoliths were prepared as described previously,[6] and pore size distributions were measured with nitrogen adsorption and desorption isotherms.[18] The monoliths

* To whom correspondence should be addressed. E-mail: fourkas@umd.edu.

10.1021/jp051384o CCC: $30.25
Published on Web 06/15/2005

were disks of approximately 6 mm diameter that were polished on both sides to a thickness of slightly less than 2 mm. Monoliths of different average pore sizes were placed in a cuvette with a 2 mm path length and immersed in liquid. Once the sol−gel samples had filled completely with liquid, enough additional liquid was added to ensure that the samples would remain submerged. The cell was then sealed. Surface modification was accomplished by refluxing the monoliths for 72 h in a 50% solution of trimethylchlorosilane in dry toluene prior to placing the monoliths in a sample cell.[19]

The OKE setup employed was similar to ones we have described previously,[16] and so we will give only a brief description of it here. A solid-state laser (Coherent Verdi 5) is used to pump a commercial Ti:sapphire laser (KMLabs TS), producing 50-fs pulses with a center wavelength of about 800 nm at a repetition rate of 76 MHz. The laser output is divided into pump and probe beams, each of which passes through a different ring of a chopper wheel. The pump beam is polarized vertically and is focused into the sample with an achromatic lens. The pump beam is picked off after the sample and focused into a doubling crystal. The frequency doubled light is collected with a photodiode, the output of which is sent to a lock-in amplifier that is referenced to the chopping frequency of the pump beam. The doubled light has the same nonlinearity as the signal of interest, allowing us to compensate for any long-term drift of the laser intensity.

The probe beam traverses an optical delay line, and then is sent through a polarizer set to pass light at a polarization angle of 45°, followed by a quarter-wave plate with its fast axis also set at 45°. The probe beam is then focused onto the same spot of the sample as is the pump beam, using the same lens. When taking data on a sol−gel sample, we ensure that the beams overlap only within the monolith so that there is no signal from the surrounding bulk liquid. The probe beam is recollimated after the sample and sent into a polarizer set to pass light with a polarization angle of −45°. With the pump beam blocked, the sample is translated to find a spot with minimal static birefringence. Once the pump beam is unblocked, the light that is transmitted through the second polarizer is spatially filtered and then collected by a low-noise, amplified photodiode. To collect data, the first polarizer in the probe beam path is rotated by approximately 1° to create a local oscillator for optical heterodyne detection.[24] In successive scans the direction of this small rotation is reversed, and the scans at opposite angles are subtracted from one another to remove any remaining homodyne contribution to the signal.

A small portion of the probe beam is picked off before the delay line and detected by an amplified photodiode that is identical with the one collecting the signal. The two photodiode outputs are sent to the two inputs of an analogue preamplifier, and are carefully matched in intensity with the pump beam blocked. The difference in signal from the two photodiodes is then amplified and sent to a lock-in amplifier that is referenced to the sum of the pump and probe chopping frequencies. A computer is used to scan the delay line, rotate the polarizer in the probe beam, and collect and average data from the two lock-in amplifiers as a function of delay time τ. All data reported here were collected at a temperature of 293 K.

All data sets were averages of at least eight scans. Since the OKE signal is the negative time derivative of the orientational correlation function,[31] the negative integral of the averaged data sets was taken, which served to smooth out any high-frequency noise. The constant of integration for each data set was determined by ensuring that the decay was exponential at long

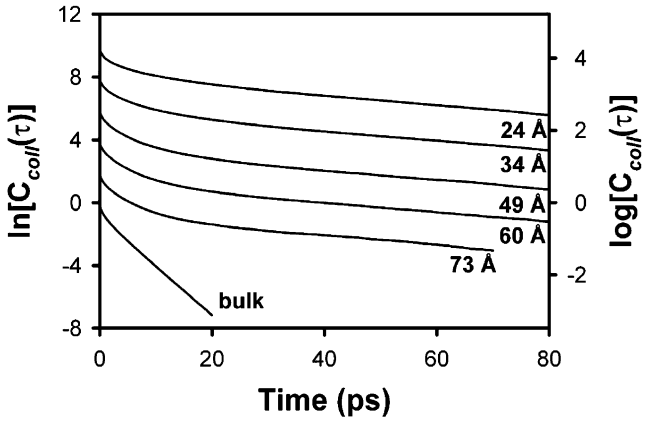

Figure 1. Collective orientational correlation functions for benzene in the bulk (bottom trace) and, from top to bottom, confined in 24, 34, 49, 60, and 73 Å pores. All data were obtained at 293 K and the correlation functions have been offset for clarity.

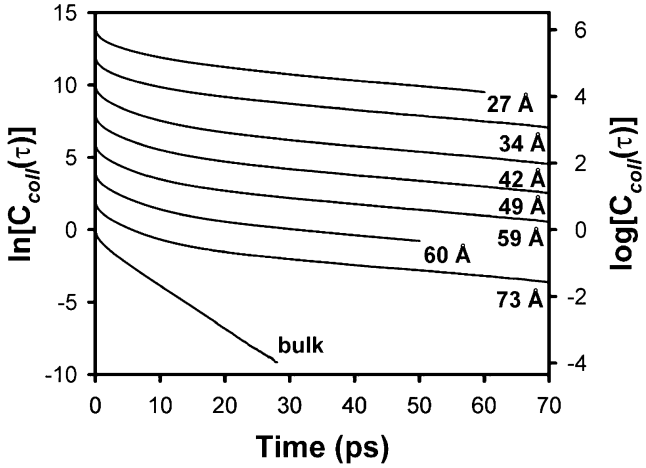

Figure 2. Collective orientational correlation functions for benzene-d_6 in the bulk (bottom trace) and, from top to bottom, confined in 27, 34, 42, 49, 59, 60, and 73 Å pores. All data were obtained at 293 K and the correlation functions have been offset for clarity.

times. Fits were made to data at decay times greater than 5 ps, at which point the signal is dominated by orientational diffusion. Fitting was performed by using a commercial software package (Systat SigmaPlot 9.0). In all cases, a biexponential function was found to provide an excellent fit to the data.

III. Results

The collective orientational correlation functions ($C_{\mathrm{coll}}(\tau)$, where τ is the delay time between the pulses) derived from the OKE decays for benzene in the bulk and in nanoconfinement in unmodified sol−gel monoliths are shown in Figure 1, and the corresponding correlation functions for benzene-d_6 are shown in Figure 2. In all cases the decays in confinement are considerably slower than those in the bulk liquid. The average decay time becomes longer as the average pore diameter decreases.

In nanoconfined weakly wetting liquids that we have studied previously, OKE data could be fit to a sum of exponentials.[6,7,9,11,17] In all cases, the time constant of the fastest of these exponentials matched well to the diffusive orientational decay of the bulk liquid. This decay has been ascribed to molecules that reside in the centers of the pores, and hence are not influenced by confinement. The slower portions of the decays were assigned to molecules at the pore surfaces with retarded orientational dynamics.

TABLE 1: Fit Parameters and Surface Layer Thickness for Benzene in Unmodified Pores[a]

pore diameter (Å)	A_1	τ_1 (ps)	A_2	τ_2 (ps)	R_s (Å)
24	0.64	6.2	0.36	33.3	2.4
34	0.74	5.5	0.26	33.3	2.4
49	0.82	4.9	0.18	33.3	2.3
60	0.84	4.3	0.16	33.3	2.5
73	0.86	4.0	0.14	33.3	2.6
bulk	1	3.19			

[a] Uncertainties are approximately ±5% for A_1 and A_2, ±5% for τ_1, ±10% for τ_2, and ±20% for R_s.

TABLE 2: Fit Parameters and Surface Layer Thickness for Benzene-d_6 in Unmodified Pores[a]

pore diameter (Å)	A_1	τ_1 (ps)	A_2	τ_2 (ps)	R_s (Å)
27	0.67	5.2	0.33	24.8	2.4
34	0.71	4.7	0.29	24.8	2.7
42	0.81	4.6	0.19	24.8	2.1
49	0.81	4.5	0.19	24.8	2.4
59	0.81	4.4	0.19	24.8	3.0
60	0.84	4.2	0.16	24.8	2.5
73	0.86	4.0	0.14	24.8	2.7
bulk	1	3.36			

[a] Uncertainties are approximately ±5% for A_1 and A_2, ±5% for τ_1, ±10% for τ_2, and ±20% for R_s.

In analogy with these previous results, the correlation functions of the confined liquids in Figures 1 and 2 can be described well by the sum of two exponentials. In unconstrained fits, the time constant of the faster exponential (τ_1) was found to depend on pore size, becoming larger as the pore size decreases for both liquids. However, the time constants for the slower decay (τ_2) were similar for all pore sizes for a given liquid, although they differed between the two liquids. There was no trend observed in the variation of this decay constant with pore size. We therefore took the average value of this decay time in all the different pore sizes for each liquid, and then refit the data with the longer decay time constrained to this value but with the constant of integration allowed to float in the nonlinear least-squares fit. In all cases the constant of integration did not change significantly when the slower decay time was constrained. The decay constants and corresponding normalized amplitudes (A_1 and A_2) for these fits are given in Tables 1 and 2, and the dependence of τ_1 on pore curvature is plotted for both liquids in Figure 3.

If we assume that τ_2 arises from reorientation of molecules at the pore surfaces and τ_1 from molecules in the centers of the pores, then the amplitudes of these two exponentials reflect the relative populations of molecules with these dynamics. We can then estimate the thickness of the surface layer with retarded reorientational dynamics using the equation[6]

$$R_s = R(1 - \sqrt{A_1}) \quad (1)$$

where R is the pore radius and R_s is the surface layer thickness. The values of R_s determined from this equation are given in Tables 1 and 2 and are plotted in Figure 4 as a function of pore diameter for both liquids. Within the margin of error in determining R_s, it takes on the same value for both liquids regardless of pore size. The average value of these measurements is 2.5 Å, or about the thickness of one benzene molecule.

In Figure 5 we illustrate typical effects that the addition of methyl groups to the pore surfaces have on the dynamics of confined benzene and benzene-d_6 by comparing the OKE decays for the former liquid in unmodified and methylated pores with 34 Å diameters. Methylation does not lead to qualitative differences in the OKE decays beyond a modest rate enhancement. The decays can still be described well by the sum of two exponentials, one with a decay time (τ_1) that is slightly larger

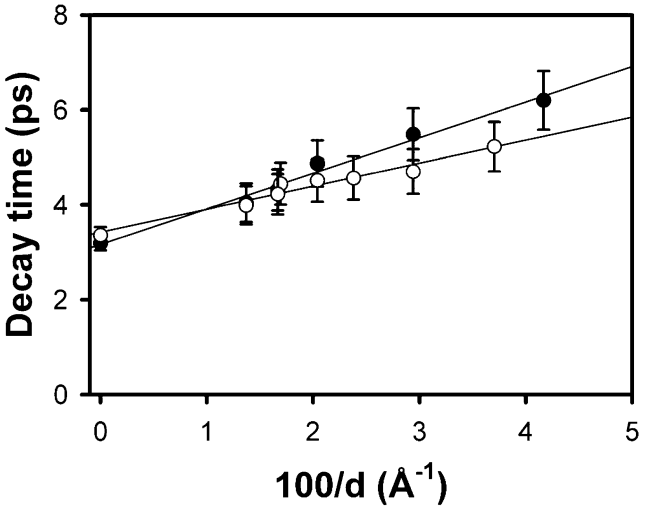

Figure 3. Fastest decay time (τ_1) as a function of the pore curvature (inverse of the pore diameter) for benzene (solid circles) and benzene-d_6 (open circles). The data points at zero curvature are for the bulk liquids, and the lines are linear least-squares fits to the data.

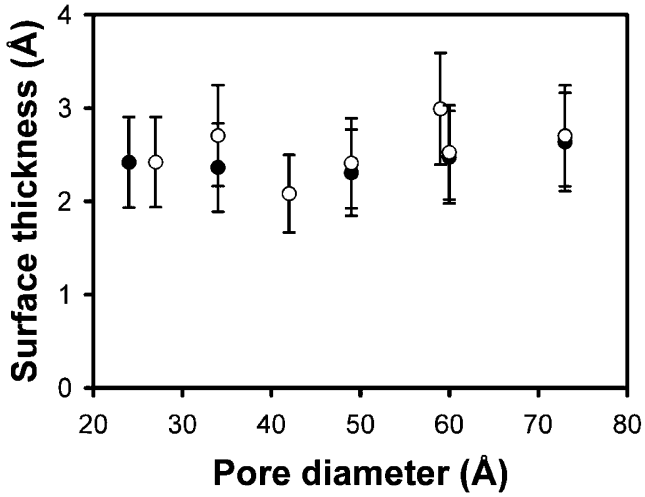

Figure 4. Calculated surface-layer thickness for benzene (solid circles) and benzene-d_6 (open circles) as a function of pore diameter.

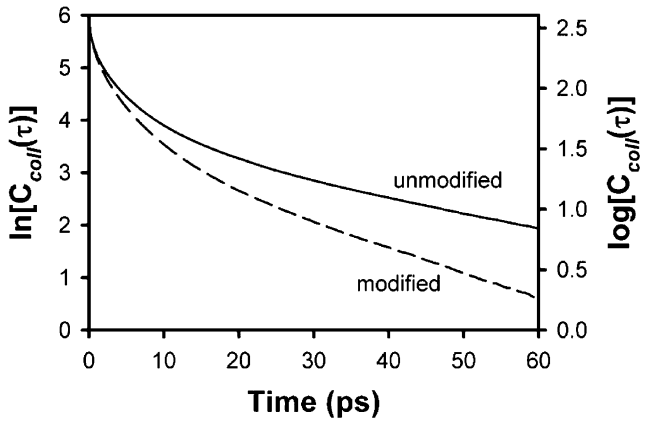

Figure 5. Representative OKE decays for benzene in 34-Å pores that are untreated (solid line) and that have surface methyl groups (dashed line).

TABLE 3: Fit Parameters and Surface Layer Thickness for Benzene in Modified Pores[a]

pore diameter (Å)	A_1	τ_1 (ps)	A_2	τ_2 (ps)	R_s (Å)
24	0.69	5.0	0.31	20.6	2.3
34	0.79	4.5	0.21	20.6	1.9
42	0.85	4.0	0.15	20.6	1.6
59	0.85	4.0	0.15	20.6	2.3
60	0.87	3.8	0.13	20.6	1.9
73	0.91	3.8	0.09	20.6	1.6
bulk	1	3.19			

[a] Uncertainties are approximately ±5% for A_1 and A_2, ±5% for τ_1, ±10% for τ_2, and ±20% for R_s.

TABLE 4: Fit Parameters and Surface Layer Thickness for Benzene-d_6 in Modified Pores[a]

pore diameter (Å)	A_1	τ_1 (ps)	A_2	τ_2 (ps)	R_s (Å)
27	0.72	4.8	0.28	19.6	2.0
34	0.76	4.2	0.24	19.6	2.2
42	0.87	4.3	0.13	19.6	1.5
49	0.85	4.0	0.15	19.6	1.9
59	0.85	4.0	0.15	19.6	2.2
60	0.89	4.0	0.11	19.6	1. 7
73	0.91	3.8	0.09	19.6	1.7
bulk	1	3.36			

[a] Uncertainties are approximately ±5% for A_1 and A_2, ±5% for τ_1, ±10% for τ_2, and ±20% for R_s.

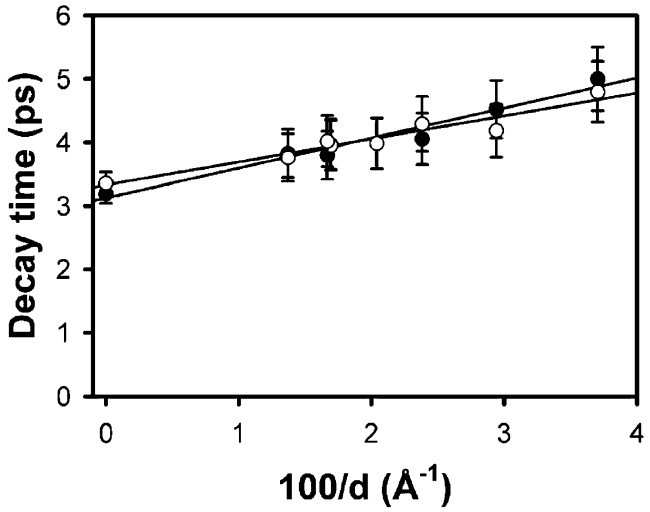

Figure 6. Fastest decay time (τ_1) as a function of the pore curvature (inverse of the pore diameter) for benzene (solid circles) and benzene-d_6 (open circles) in pores with surface methyl groups. The data points at zero curvature are for the bulk liquids, and the lines are linear least-squares fits to the data.

than the bulk relaxation time and that increases with decreasing pore size and one with a decay time (τ_2) that is significantly larger than the bulk decay time and does not depend on pore size. The decay constants and normalized amplitudes for these fits are given in Tables 3 and 4. The values of τ_1 as a function of pore curvature are plotted for both liquids in Figure 6. As in the case of the unmodified pores, this decay time depends roughly linearly on pore curvature. It is also worth noting that due to methylation, the true pore diameters must be somewhat smaller than the values given, which were measured in the untreated samples. Finally, the surface layer thickness is plotted as a function of pore size for both liquids in Figure 7; in each case, the average value of the thickness is about 1.9 Å.

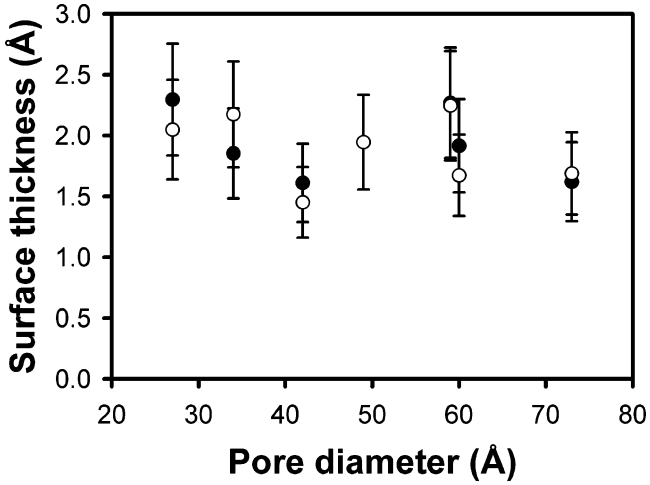

Figure 7. Calculated surface-layer thickness for benzene (solid circles) and benzene-d_6 (open circles) as a function of pore diameter in pores with surface methyl groups.

IV. Discussion

The behavior of these liquids in unmodified pores differs from what we have observed previously for weakly wetting liquids composed of rodlike molecules[6,7,11,17] in at least two significant aspects. First, while there is a clear bulklike component in the orientational dynamics of weakly wetting confined liquids such as CS_2 and 2-butyne, no relaxation component is observed in benzene or benzene-d_6 with a decay time that matches that of the bulk liquid. However, as can be seen in Figure 3, τ_1 for benzene and benzene-d_6 varies linearly with pore curvature and is equal to the bulk relaxation time in the limit of zero curvature. Second, the surface relaxation of benzene and benzene-d_6 is, within the accuracy of our measurements, independent of pore size. This observation rules out any significant influence of the geometric effects that inhibit surface reorientation in weakly wetting liquids such as CS_2 and 2-butyne. On the other hand, τ_2 is up to an order of magnitude greater than τ_1, which is too large for an increase in the hydrodynamic volume for reorientation to be responsible for the retardation of orientational dynamics at pore surfaces.

Undoubtedly much of the explanation for the differences between the dynamics of confined benzene and those of liquids such as CS_2 and 2-butyne lies in the fact that while benzene neither has a dipole moment nor can accept hydrogen bonds, it nevertheless wets silica surfaces strongly. Indeed, the contact angle of benzene on glass is approximately 6°.[32] The interactions between benzene and silica surfaces arise through a combination of electrostatic interactions (via the substantial quadrupole moment of benzene[33]), dispersion interactions, and cation-π interactions[34] with the protons of the surface hydroxyl groups (both of which rely on the sizable polarizability of benzene). All of these interactions are likely to favor benzene lying flat on the pore surfaces. Thus, the relatively large surface reorientation times in all likelihood can be ascribed to the significant energy required to remove benzene from the surfaces, rather than to geometric or hydrodynamic volume effects. This interpretation is further supported by the fact that the surface layer thickness is on the order of the thickness of a benzene molecule but is substantially less than its diameter.

Given that benzene wets silica strongly, it is appropriate to compare its dynamics in confinement to those of other strongly wetting liquids. We have previously used OKE spectroscopy to study the orientational dynamics of acetonitrile and acetonitrile-d_3 confined in nanoporous glasses.[8,12] The molecules of

these liquids are able to accept hydrogen bonds from the surface hydroxyl groups of silica, and so wet the pore surfaces strongly. The OKE decays for these liquids are triexponential. The fastest of the three time constants matches that of the bulk liquid. The other two time constants are independent of pore size at a given temperature, although the relative amplitudes of the three exponentials do change with pore size. We have interpreted these results in terms of a bulklike population of molecules in the pore centers and a population that experiences dynamic inhibition at the pore surfaces.[8,12] We have been able to explain the data with a model in which exchange of molecules off of the pore surfaces into the bulklike population is an additional channel for surface relaxation. Roughly half of the molecules at the pore surfaces undergo orientational relaxation without exchanging, whereas the remaining surface molecules do exchange into the bulk. Deuterium exchange on the surface hydroxyl groups does not change the observed dynamics,[12] suggesting that the nonexchanging surface molecules are tethered by hydrogen bonds whereas the exchanging molecules are not.

There are two important differences between the dynamics of confined benzene and those of confined acetonitrile. First, confined benzene has no relaxation component that decays at the bulk rate. Second, there is no sign of exchange of molecules off of the surface in the benzene data. The second of these differences can be explained by the differences in surface interactions between the two liquids. We believe that the orientational dynamics of acetonitrile molecules that are near, but not bound to, the pore surfaces are constrained by the dynamics of their neighbors that are bound to the surfaces. However, these unbound molecules are capable of exchanging into the bulklike component of the liquid. The molecules that are bound to the surface, on the other hand, relax while remaining tethered to the surface. In the case of benzene, molecules that are lying flat on the surface cannot reorient about an axis in the plane of the disk (the only type of motion to which OKE spectroscopy is sensitive) without coming off of the surface. In this sense, reorientation and exchange of surface-bound molecules are essentially the same process.

The only liquid that we have studied previously that has not exhibited a relaxation component at the bulk rate in confinement is water.[15] Even in pores with a diameter of 100 Å, there is no sign of such relaxation in confined water. We believe that nanoconfinement has such a profound effect on the orientational dynamics of water because this liquid is so highly networked. While a highly hydrogen-bonded liquid such as water would not seem to be a good point of comparison for the data presented here, simulations and scattering data suggest that benzene is in fact a relatively highly ordered liquid.[35,36] Due to the sizable quadrupole moment of the benzene molecules, they tend to form local T-shaped structures.[35,36] This motif is also observed in benzene crystals,[37] which feature a herringbone-like pattern of molecules. Because molecules will tend to lie flat on the pore surfaces, the liquid structure may be disrupted significantly. Furthermore, the slow orientational dynamics of these surface molecules can exert an effect over large distances via this networked T structuring.

It is also worthy of note that the surface relaxation times of benzene and benzene-d_6 differ from one another significantly. Although benzene relaxes somewhat more quickly than does benzene-d_6 in the bulk (3.19 ps versus 3.36 ps at 293 K), the surface relaxation time for benzene is approximately 33 ps, while that of benzene-d_6 is approximately 25 ps. While the uncertainty in each surface relaxation time is on the order of $\pm 10\%$, it proved to be impossible to fit both the benzene and benzene-d_6 data with the same surface relaxation time, and so we are confident that this difference in surface relaxation times is real. We note also that the pore-size dependence of τ_1 for benzene-d_6 is somewhat milder than that for benzene.

The differences in the surface relaxation times of these two liquids are probably related to differences in surface energies on silica. Since C−D bonds are somewhat shorter than C−H bonds, both the polarizability and the quadrupole moment of benzene-d_6 are slightly smaller than those of benzene. This leads to benzene-d_6 having a somewhat smaller surface tension than benzene,[38] and presumably also leads to benzene-d_6 having weaker interactions with the pore surfaces (it is difficult to measure any difference between the contact angles of the two liquids on silica as these angles are so small). The faster surface relaxation of benzene-d_6 can in turn lead to faster relaxation in the pore centers as compared to benzene as well.

We now turn to the dynamics of these liquids in modified pores. Benzene wets solid, saturated hydrocarbons well, and so could have interactions with the methylated surfaces that are comparable to those with unmodified silica surfaces. Indeed, contact angle measurements of benzene and benzene-d_6 on methylated cover slips revealed contact angles in the range of 13°, which is larger than the 6° contact angle on unmodified cover slips. This corresponds to enough of a difference in surface energy that the surface relaxation in modified pores is significantly faster than that in unmodified pores, although it is still much slower than that in the bulk. As a result, the relaxation of the remaining confined molecules is faster than that in unmodified pores as well. Furthermore, as shown by Figure 7 the apparent surface layer thickness is markedly smaller after the pores have been modified. In addition, because modification makes the pore diameters smaller to some extent, the difference in surface layer thickness is probably even greater than what we have estimated. We can draw an analogy here to weakly wetting liquids, in which we have also observed submonolayer populations of dynamically inhibited molecules. Our interpretation in these weakly wetting systems is that only molecules that lie flat on the pore surfaces exhibit additional dynamic inhibition. This model would suggest that benzene has less of a tendency to lie flat on methyl modified surfaces than on unmodified silica. In other words, the face of a benzene molecule is more "hydrophilic" and the edges are more "hydrophobic". This idea could be tested with surface sum-frequency generation experiments.[39−41]

A comparison of our results to dielectric spectroscopy studies on networked liquids in pores is also informative. Kremer and co-workers have studied the dynamics of hydrogen-bonding supercooled liquids in modified and unmodified pores with broadband dielectric spectroscopy.[42−45] In unmodified pores a bound surface layer with inhibited dynamics has been observed; as in our experiments with acetonitrile, exchange of molecules off of the pore surfaces is an important channel for surface relaxation.[42,43] In these experiments the molecules have specific interactions (hydrogen bonds) with unmodified pore surfaces that can be altered by silanization. Indeed, in modified pores the dynamics become similar to those of the bulk liquid.[44] As discussed above, benzene wets both modified and unmodified surfaces well, and so the differences in the different pores are considerably smaller. It is interesting that the effects of confinement on the benzene molecules that are not near the pore walls are stronger than the effects of confinement on hydrogen-bonding liquids in the pore centers, even though benzene is not generally considered a networked liquid.

TABLE 5: Comparison of Raman and OKE Data for Benzene-d_6 in Unmodified Pores[a]

pore diameter (Å)	τ_{Raman} (ps)	$\tau_{Raman,corr}$ (ps)	$\langle\tau_{OKE}\rangle$ (ps)	$\langle g_2\rangle$	$g_{2,surface}$
27	4.9	8.7	11.6	1.3	1.5
34	4.3	7.6	10.6	1.4	1.7
42	3.9	6.8	8.4	1.2	1.5
49	3.6	6.3	8.3	1.3	1.7
59	3.3	5.8	8.4	1.4	2.1
60	3.3	5.8	7.5	1.3	1.8
73	3.0	5.4	6.9	1.3	1.8
bulk	1.9	3.36	3.36	1.0	

[a] Uncertainties are approximately ±5% for τ_{Raman} and $\tau_{Raman,corr}$, ±10% for $\langle\tau_{OKE}\rangle$, ±10% for $\langle g_2\rangle$, and ±10% for $g_{2,surface}$.

It is also interesting to compare our results to those of Yi and Jonas,[46] who used Raman spectroscopy to study the dynamics of orientational diffusion of benzene-d_6 in the same type of monolithic porous glasses. The orientational correlation time measured in these experiments, τ_{Raman}, was also found to vary linearly with pore curvature.[46] Based on this linear fit, we have tabulated in Table 5 the values of τ_{Raman} that would be expected for the pore diameters used in our benzene-d_6 OKE experiments.

There are two important differences between the OKE and Raman measurements in this system. First, the Raman experiments were used to measure average orientational correlation times rather than the orientational correlation function, and so τ_{Raman} effectively averages over all of the dynamic environments in the pores. Second, while OKE experiments measure a collective orientational correlation time, Raman experiments measure a single-molecule orientational correlation time. Given a single dynamic population of molecules, these two times are related by[47]

$$\tau_{OKE} = \frac{g_2}{j_2}\tau_{Raman} \tag{2}$$

where g_2 and j_2 are respectively the static and dynamic pair orientational correlation parameters. In liquids j_2 is generally believed to be unity,[47] and so g_2 is assumed to be the constant of proportionality between the OKE and Raman orientational correlation times. The static pair orientational correlation parameter can take on values of unity or greater, with larger values corresponding to a greater degree of parallel ordering among molecules in the liquid.

In benzene, g_2 takes on a value of approximately unity,[23,48] which is presumably in part a result of the propensity of this liquid to form T-shaped structures.[36] Benzene-d_6 should have a value of g_2 that is similar to that of benzene, and yet the values of τ_{Raman} and τ_{OKE} for the bulk liquid differ considerably. If we assume that there is a systematic difference between the two, then we can calculate a corrected Raman correlation time $\tau_{Raman,corr}$ by multiplying τ_{Raman} by the ratio of τ_{OKE} to τ_{Raman} in the bulk liquid. The values of $\tau_{Raman,corr}$ for the different pore sizes are also listed in Table 5.

To compare our OKE data to the corrected Raman data, we compute an average OKE relaxation time $\langle\tau_{OKE}\rangle$ using

$$\langle\tau_{OKE}\rangle = A_1\tau_1 + A_2\tau_2 \tag{3}$$

This average value can in turn be used in conjunction with $\tau_{Raman,corr}$ to estimate the average value of the static pair orientational correlation parameter, $\langle g_2\rangle$, for each pore size. Both $\langle\tau_{OKE}\rangle$ and $\langle g_2\rangle$ are tabulated in Table 5. It can be seen from these results that $\langle g_2\rangle$ takes on a value near 1.3 in confinement,

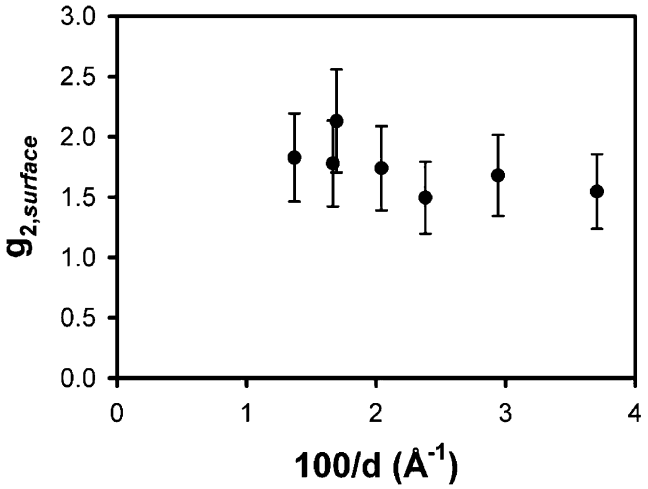

Figure 8. Estimated values of $g_{2,surface}$ as a function of pore curvature.

which points to an increased degree of parallel alignment in the pores. However, there is little reason to believe that in the centers of the pores g_2 should differ significantly from its bulk value, particularly when the pore diameter is large. If we assume that g_2 can take on different values for the surface and bulklike populations of confined molecules, then the corrected Raman correlation time can be written as

$$\tau_{Raman,corr} = \frac{A_1\tau_1}{g_{2,bulklike}} + \frac{A_2\tau_2}{g_{2,surface}} \tag{4}$$

If we further assume that $g_{2,bulklike}$ is unity, then we find that

$$g_{2,surface} = \frac{A_2\tau_2}{\tau_{Raman,corr} - A_1\tau_1} \tag{5}$$

Values of $g_{2,surface}$ estimated in this manner are tabulated in Table 5.

The values of $g_{2,surface}$ suggest that there is significant parallel ordering of benzene-d_6 on the pore surfaces, which is consistent with the idea that the molecules tend to lie flat on the pore walls. This result is also in line with the results of previous experiments on confined acetonitrile.[12] It is apparent from these data that the degree of surface ordering increases with increasing pore size, which at first might seem surprising. It is possible that the surface relaxation time does depend somewhat on pore curvature, but that the dependence is too subtle for us to detect without data of even higher quality. Any such dependence of τ_2 on pore curvature could not be great enough to account for the observed variation of $g_{2,surface}$, however. On the other hand, while the molecules may lie flat on the pore surfaces, since the surfaces themselves are not flat the surface molecules are not necessarily parallel to one another. Indeed, in more tightly curved pores it would be expected that there would be less parallel surface ordering. In Figure 8 we plot the estimated value of $g_{2,surface}$ as a function of pore curvature. The dependence on pure curvature is roughly linear, and if we extend a linear fit out to zero curvature we find a value near 2. This extrapolation suggests that there is nearly perfect parallel alignment at a flat surface, which is consistent with benzene molecules lying flat on silica.

V. Conclusions

We have presented a detailed study of the orientational dynamics of benzene and benzene-d_6 confined in nanoporous glasses, both with silica surface and with methylated surfaces.

In all cases the observed dynamics can be described well by the sum of two exponentials, one with a time constant that is somewhat longer than that for the bulk liquid and that depends on the pore size and the other with a much longer time constant that does not depend on pore size. We have assigned these two exponentials to bulklike molecules in the pore centers and surface molecules, respectively. The slow surface relaxation is indicative of strong interactions between the liquid and the pore surfaces, which is consistent with the results of contact angle measurements. In the unmodified pores, the surface layer has the thickness of about one benzene molecule, which suggests that the benzene molecules lie flat on the pore surfaces. Comparison with Raman data supports this picture. Although benzene is not a networked liquid, in the centers of the pores its reorientational dynamics are still strongly influenced by confinement, which is reminiscent of what we have seen in confined water and suggests that benzene retains strong ordering in the nanopores. It will be of great interest to extend these studies to other confined aromatic systems and to make further comparisons with single-molecule orientational data.

Acknowledgment. This work was supported by the National Science Foundation, Grant CHE-0314020. J.T.F. is a Research Corporation Cottrell Scholar and a Camille Dreyfus Teacher−Scholar.

References and Notes

(1) *Molecular Dynamics in Restricted Geometries*; Drake, J. M., Klafter, J., Eds.; Wiley: New York, 1989.

(2) *Dynamics in Small Confining Systems*; Drake, J. M., Klafter, J., Kopelman, R., Awschalom, D. D., Eds.; Materials Research Society: Pittsburgh, PA, 1993; Vol. 290, p 377.

(3) *Dynamics in Small Confining Systems II*; Drake, J. M., Klafter, J., Kopelman, R., Troian, S. M., Eds.; Materials Research Society: Pittsburgh, PA, 1995; Vol. 366, p 466.

(4) *Dynamics in Small Confining Systems III*; Drake, J. M., Klafter, J., Kopelman, R., Eds.; Materials Research Society: Pittsburgh, PA, 1997; Vol. 464, p 388.

(5) *Dynamics in Small Confining Systems IV*; Drake, J. M., Grest, G. S., Klafter, J., Kopelman, R., Eds.; Materials Research Society: Warrendale, PA, 1999; Vol. 543, p 372.

(6) Farrer, R. A.; Loughnane, B. J.; Fourkas, J. T. *J. Phys. Chem. A* **1997**, *101*, 4005.

(7) Loughnane, B. J.; Farrer, R. A.; Deschenes, L. A.; Fourkas, J. T. Temperature-Dependent Dynamics of Microconfined CS_2. In *Dynamics in Small Confining Systems III*; Drake, J. M., Klafter, J., Kopelman, R., Eds.; Materials Research Society: Pittsburgh, PA, 1997; Vol. 464, p 263.

(8) Loughnane, B. J.; Farrer, R. A.; Fourkas, J. T. *J. Phys. Chem. B* **1998**, *102*, 5409.

(9) Loughnane, B. J.; Fourkas, J. T. *J. Phys. Chem. B* **1998**, *102*, 10288.

(10) Loughnane, B. J.; Farrer, R. A.; Fourkas, J. T. Rotational Diffusion of Microconfined Liquids. In *Dynamics in Small Confining Systems IV*; Materials Research Society: Pittsburgh, PA, 1999; p 33.

(11) Loughnane, B. J.; Scodinu, A.; Fourkas, J. T. *J. Phys. Chem. B* **1999**, *103*, 6061.

(12) Loughnane, B. J.; Farrer, R. A.; Scodinu, A.; Fourkas, J. T. *J. Chem. Phys.* **1999**, *111*, 5116.

(13) Loughnane, B. J.; Scodinu, A.; Fourkas, J. T. *Chem. Phys.* **2000**, *253*, 323.

(14) Loughnane, B. J.; Farrer, R. A.; Scodinu, A.; Reilly, T.; Fourkas, J. T. *J. Phys. Chem. B* **2000**, *104*, 5421.

(15) Scodinu, A.; Fourkas, J. T. *J. Phys. Chem. B* **2002**, *106*, 10292.

(16) Farrer, R. A.; Fourkas, J. T. *Acc. Chem. Res.* **2003**, *36*, 605.

(17) Scodinu, A.; Farrer, R. A.; Fourkas, J. T. *J. Phys. Chem. B* **2002**, *106*, 12863.

(18) Brinker, C. J.; Scherer, G. W. *Sol−Gel Science*: *The Physics and Chemistry of Sol−Gel Processing*; Academic Press: San Diego, CA, 1990.

(19) Majors, R. E.; Hopper, M. J. *J. Chromatogr. Sci.* **1974**, *12*, 767.

(20) Righini, R. *Science* **1993**, *262*, 1386.

(21) Fourkas, J. T. Nonresonant Intermolecular Spectroscopy of Liquids. In *Ultrafast Infrared and Raman Spectroscopy*; Fayer, M. D., Ed.; Marcel Dekker: New York, 2001; Vol. 26, p 473.

(22) Kinoshita, S.; Kai, Y.; Ariyoshi, T.; Shimada, Y. *Int. J. Mod. Phys. B* **1996**, *10*, 1229.

(23) Loughnane, B. J.; Scodinu, A.; Farrer, R. A.; Fourkas, J. T.; Mohanty, U. *J. Chem. Phys.* **1999**, *111*, 2686.

(24) McMorrow, D.; Lotshaw, W. T. *J. Phys. Chem.* **1991**, *95*, 10395.

(25) Chang, Y. J.; Castner, E. W., Jr. *J. Phys. Chem.* **1996**, *100*, 3330.

(26) Neelakandan, M.; Pant, D.; Quitevis, E. L. *Chem. Phys. Lett.* **1997**, *265*, 283.

(27) Ricci, M.; Bartolini, P.; Chelli, R.; Cardini, G.; Califano, S.; Righini, R. *Phys. Chem. Chem. Phys.* **2001**, *3*, 2795.

(28) Chelli, R.; Cardini, G.; Ricci, M.; Bartolini, P.; Righini, R.; Califano, S. *Phys. Chem. Chem. Phys.* **2001**, *3*, 2803.

(29) Ratajska-Gadomska, B.; Gadomski, W.; Wiewior, P.; Radzewicz, C. *J. Chem. Phys.* **1998**, *108*, 8489.

(30) Ricci, M.; Wiebel, S.; Bartolini, P.; Taschin, A.; Torre, R. *Philos. Mag.* **2004**, *84*, 1491.

(31) Berne, B. J.; Pecora, R. *Dynamic Light Scattering*; Wiley: New York, 1976.

(32) Irons, E. J. *Philos. Mag.* **1943**, *34*, 614.

(33) Battaglia, M. R.; Buckingham, A. D.; Williams, J. H. *Chem. Phys. Lett.* **1981**, *78*, 421.

(34) Ma, J. C.; Dougherty, D. A. *Chem. Rev.* **1997**, *97*, 1303.

(35) Narten, A. H. *J. Chem. Phys.* **1977**, *67*, 2102.

(36) Cabaco, M. I.; Danten, Y.; Besnard, M.; Guissani, Y.; Guillot, B. *J. Phys. Chem. B* **1997**, *101*, 6977.

(37) Bacon, G. E.; Curry, N. A.; Wilson, S. A. *Proc. R. Soc. A* **1964**, *279*, 98.

(38) Gaines, G. L., Jr.; Le Grand, D. G. *Colloids Surf. A* **1994**, *82*, 299.

(39) Eisenthal, K. B. *Chem. Rev.* **1996**, *96*, 1343.

(40) Richmond, G. L. *Annu. Rev. Phys. Chem.* **2001**, *52*, 357.

(41) Richmond, G. L. *Chem. Rev.* **2002**, *102*, 2693.

(42) Arndt, M.; Stannarius, R.; Gorbatschow, W.; Kremer, F. *Phys. Rev. E* **1996**, *54*, 5377.

(43) Gorbatschow, W.; Arndt, M.; Stannarius, R.; Kremer, F. *Europhys. Lett.* **1996**, *35*, 719.

(44) Arndt, M.; Stannarius, R.; Groothues, H.; Hempel, E.; Kremer, F. *Phys. Rev. Lett.* **1997**, *79*, 2077.

(45) Huwe, A.; Arndt, M.; Kremer, F.; Haggenmuller, C.; Behrens, P. *J. Chem. Phys.* **1997**, *107*, 9699.

(46) Yi, J.; Jonas, J. *J. Phys. Chem.* **1996**, *100*, 16789.

(47) Kivelson, D.; Madden, P. A. *Annu. Rev. Phys. Chem.* **1980**, *31*, 523.

(48) Madden, P. A.; Battaglia, M. R.; Cox, T. I.; Pierens, R. K.; Champion, J. *Chem. Phys. Lett.* **1980**, *76*, 604.